Shock Tunnel Measurements of Heat Transfer in a Model Scramjet

R.G. Morgan* and R.J. Stalker†
University of Queensland, St. Lucia, Australia

The results of heat-transfer measurements to the walls of a two-dimensional scramjet combustion chamber in a shock tunnel are presented. Thin-film heat-transfer gages on a ceramic glass substrate were used. The range of experimental conditions covered produced boundary layers ranging from laminar to transitional, as was independently checked by flow visualization. Empirical flat-plate correlations, corrected for local pressure disturbances, were used to make a comparison with the experimental results. In the fully laminar regime, the heating rates were found to give approximate agreement with the empirical estimates. In the nonlaminar tests, the heating rate is found to be well below the fully turbulent levels. It is not known at present if this is a transition effect or if the pressure-corrected flat-plate turbulent correlations do not apply to the configuration used.

Nomenclature

h = static enthalpy
H = total enthalpy
M = Mach number
N_{ST} = Nusselt number
P = static pressure
P_r = Prandtl Number
$\dot{q}$ = heat-transfer rate
r = recovery factor
Re = Reynolds number
St = Stanton number
T = temperature
u = velocity
x = wetted length measured from intake
α = dissociation fraction of oxygen

Subscripts and Superscripts

L = local
0 = total
r = recovery
γ = ratio of specific heats
ρ = density
μ = viscosity
$*$ = reference
∞ = freestream

Introduction

A SCRAMJET (supersonic combustion ramjet) by its very nature must spend long periods of time at high speeds within the atmosphere. It will thus be subjected to significant aerodynamic heating for extended periods, causing surface cooling requirements to become an important design consideration. Therefore, it was decided to incorporate heat-transfer surveys into a series of experiments set up primarily for thurst performance measurement.

Carlson[1] has performed a detailed design study for a scramjet-powered missile for flight speeds of up to Mach 6. The insulating materials used are pushed toward their thermal limits and knowledge of the surface heating rates is therefore important. Carlson uses the same laminar empirical prediction techniques discussed in this paper. Although the data presented here are simulating higher flight speeds, questions as to the validity of the empirical correlations may be relevant.

Guy and Mackley[2] measured the heat transfer in the combustion chamber of a model scramjet and used the data to provide an indication of the point of ignition and total heat release. The emphasis of this paper is to investigate the conduction of heat across the boundary layer within the duct, with and without fuel injection.

The experiments were performed at conditions corresponding to flight speeds of 1.8-5 km/s, which cover most of the likely operating range and overlap other data available[2] for speeds up to 2.2 km/s. The shock tunnel T3 at the Australian National University[3] was used to produce the necessary test conditions. It is the only facility currently capable of producing reliable and proven test conditions at the higher enthalpies.[4]

Driver gas contamination is a potential problem for high-enthalpy shock tunnel testing. A feature of the T3 tunnel is that the mass spectrometric calibration procedure used by Crane and Stalker[5] has provided assurance that the limits of uncontaminated test time were not exceeded in the experiments.

Due to facility limitations, the present study is restricted to the combustion chamber and a small expansion region where, due to the high local temperatures and pressures, heat transfer is at a maximum.

Combustion chamber inlet pressures were between 1.2 and 1.6 atm throughout the experiments. This was sufficient to allow substantial mixing and combustion within the confines of the model. If the combustion heat release is dominated by chemical reactions that are essentially binary in nature, then, in scaling up to the larger configurations that may be typical of flight applications, both chemistry and mixing may be expected to scale as the Reynolds number. Thus, the Reynolds numbers obtained in these experiments are typical of those that might be experienced by a flight engine operating under conditions producing about the same degree of mixing and combustion.

The Experimental Facility

A two-dimensional, constant-area combustion chamber connected to a short thrust nozzle was used for the heat-transfer measurement experiments. A conical Mach 3.5 nozzle was attached to the end of the shock tube to create the required intake conditions. Hydrogen fuel was injected into the combustion chamber as a two-dimensional supersonic jet

Presented as Paper 85-0908 at the AIAA 20th Thermophysics Conference, Williamsburg, VA, June 19-21, 1985; revision submitted Dec. 16, 1985.

*Senior Research Fellow, Department of Mechanical Engineering. Member AIAA.

†Professor, Department of Mechanical Engineering. Member AIAA.

across the whole width of the duct. A schematic of the experimental rig is shown in Fig. 1; the experimental procedure is described more fully in Ref. 6. The arrangement shown here is different in that a symmetrical nozzle with two thrust surfaces was used, one instrumented with heat-transfer gages and the other with pressure transducers. This enabled the pressure and heat-transfer measurements to be obtained simultaneously over the thrust-producing regions of the model. This is necessary because it is not possible to reproduce exactly the same fuel injection conditions between runs. A pulsed hydrogen injection system[7] was used to establish a calibrated steady flow of the fuel prior to running the shock tunnel, which had a steady running time of up to 1 ms. The angle of the thrust surfaces to the incoming flow could be adjusted to give some control over the amount of expansion experienced by the combustion products. The pressure measurements were used to calculate thrust and, in this instance, also used to produce estimates of the local heat-transfer rate. The length of the constant-area section of the combustion chamber was adjustable and the results for two configurations are presented here. The diverging section started 114 and 264 mm from the intake for combustion chambers, respectively designated short and long. The thrust surfaces were inclined at 7.5 deg to the flow for both conditions. For the tests on a constant-area duct, the thrust surfaces were aligned with the incoming flow to give a long constant-area combustion chamber.

Instrumentation

Thin-film gages were used to measure the surface temperature in both the combustion chamber and thrust nozzle. These were in the form of platinum resistance thermometers, constructed according to instructions from Allen.[8] The procedure has since been documented.[9] The gages were painted onto a substrate of Dow Corning Macor machinable glass ceramic, which could be positioned as required on the thrust surface. The gages were coated in a layer of silicon monoxide to a depth of approximately 2500 Å, the purpose of which was to insulate the sensors from any conducting effects of ionization in the shock-heated test gas. Connections to the gages were made by wires inserted into holes drilled through the substrate to the rear face of the model. Gold-painted tabs, deposited in the same process as the platinum sensing element, with which it makes good electrical contact, were attached to the wires by use of a silver-loaded conducting epoxy. A schematic diagram of the attachment arrangement is shown in Fig. 2.

The gages were powered by a constant current supply, so that any change in voltage could be correlated to the change in surface temperature, as explained in Ref. 10.

To obtain heat-transfer rates from the surface temperature time history, a one-dimensional, semi-infinite solution to the unsteady internal conduction of heat within the substrate was assumed. The stored temperature signal was then analyzed digitally with a technique presented in Ref. 10 in order to calculate the heat-transfer rate.

The response of the gages to infrared radiation, which might be emitted from the combustion region, was checked by exposing the element to a pulse of radiation from a heat source at 1150 K, as measured by a hand-held infrared pyrometer. Two calibrated gages, one of which was coated with a layer of matt black paint of known absorptance to infrared, were simultaneously exposed to the radiation. The thickness of the paint layer, while such that it would produce unacceptable response times in the shock tunnel, did not introduce significant delay during the absorptance measurements, which lasted for several hundreds of milliseconds. The absorptance of a newly cleaned gage was found to be ~0.7; but, after being exposed to the shock tunnel flow, the absorptance rose to ~0.95 due to the deposition of a thin layer of dirt. The gages were therefore considered to be measuring the total heat flux, both radiated and conducted, to the wall of the scramjet.

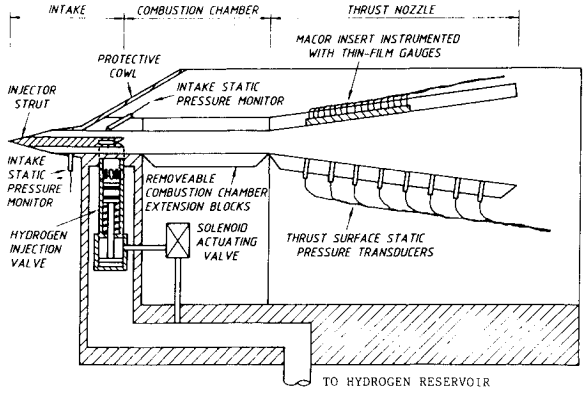

Fig. 1 Section of scramjet model with long combustion chamber.

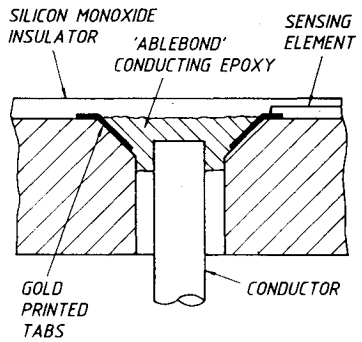

Fig. 2 Construction of heat transfer gage.

PCB pietzotronic quartz pressure transducers were used to measure the static pressure distribution over the same region, but on opposite sides of the nozzle, as covered by the heat-transfer gages. Before positioning the heat-transfer gages, pressure transducers were placed on both sides of the nozzle to confirm that the pressure distributions were symmetrical. The heat-transfer gages gave better spatial resolution than the minimum spacing of the pressure transducers permitted and were also used to confirm that there were no anomalies in the flow between the pressure transducer locations.

Test Conditions

Flow conditions at the intake of the model must be known in order to compare the experimental results with existing empirical prediction procedures. This has been done by using a nonequilibrium nozzle program[11] to expand the test gas from the assumed equilibrium conditions in the shock tube through the nozzle geometry used. The results of these computations are shown in Table 1.

The Reynolds numbers of these experiments are of a size normally associated with turbulent boundary layers. However, the boundary layer is highly cooled, a situation known to increase the stability of laminar flow.[12] Flow visualization by Mach Zehnder interferometry was used to determine the state of the boundary layer in the combustion chamber, upstream of the diverging section, for conditions A and C. No measurable boundary layer could be identified for condition A, indicating a laminar boundary layer. For condition C, the boundary layer was seen to extend for ~3 mm, which is consistent with approximate calculations for turbulent layers. There was no visualization for condition B, but the heating rates presented below suggest that it was also laminar. This is consistent with the results of Ref. 13 for cooled boundary layers at Mach 6. However, it should be noted that the wall-to-total temperature ratios are lower for the present conditions.

Table 1 Computed combustion chamber intake conditions

Condition	U, m/s	P, kPa	To, K	T_∞, K	α (oxygen)	Re_∞, m^{-1}
A	3.7	147	6500	3200	0.352	6.2×10^6
B	3.25	160	5300	2500	0.103	9.5×10^6
C	2.2	120	2950	950	0.001	2.3×10^7

Empirical Predictions

For conditions where the boundary layer is believed to be turbulent, theoretical values for the heat-transfer rates were obtained following the treatment presented in Ref. 14 for turbulent boundary layers on a flat plate. This is based on an empirical method[15] whereby the heat-transfer rate may be estimated from a knowledge of the freestream conditions and the local wall static pressure. A Lewis number of 1 and a Prandtl number of 0.72 were assumed. Transport properties must be evaluated at an effective temperature that is a defined function of the known flow conditions. This procedure has been found to give good agreement to a wide range of experimental data.

The Stanton number is determined as follows:

$$\dot{q}_w = \rho_e u_e (H_r - H_w) St_e$$

$$= \frac{0.0296}{Pr^{2/3}} \rho^* u_e (H_r - H_w) \left(\frac{\rho^* u_e \chi}{\mu^*}\right)^{-1/5} \quad (1)$$

The quantities with superscript * must be evaluated at the reference temperature T^*, defined as

$$\frac{T^*}{T_e} = \frac{1}{2}\left[\left(1+\frac{T_w}{T_0}\right) + \frac{\gamma-1}{2} M_e^2 \left(0.44r + \frac{T_w}{T_0}\right)\right] \quad (2)$$

In following this treatment, it is assumed that combustion is restricted to a limited mixing zone away from the side walls and that there is a region of isentropic flow between the mixing zone and the boundary layer on the wall. The effects of combustion are felt in the boundary layer only through the action of pressure disturbance propagating from the combustion and expansion zone to the wall and assumed to be isentropic. The conditions on the edge of the boundary layer were calculated by assuming isentropic flow from the inlet conditions to the local static pressure. Stollery and Coleman[14] used a Reynolds number based on the energy thickness to avoid having to define an origin for the turbulent bounday layer. Calculation of the energy thickness involves integrating the wall heat transfer along the boundary layer, but, as the model was not instrumented along its full length, this was not possible here. Instead, the Reynolds number was based on assumed conditions at the edge of the boundary layer and the wetted length measured from the model inlet. Because the heat flux shows only a one-fifth power dependence on Reynolds number, this is unlikely to lead to serious error.

For conditions where the boundary layer is taken to be laminar, the heating rates were estimtaed by using an empirical laminar boundary layer correlation from Ref. 16. The technique allows for the heating rate to be deduced from local static pressure measurements. The same assumptions as previously used for the turbulent case were made for conditions at the edge of the boundary layer. The laminar heat-transfer rate is given by

$$q = 0.332\sqrt{\frac{\rho^*\mu^*}{\rho\mu}} R_{e_{xL}}^{-1/2} P_r^{*-2/3} \rho_e u_e (H_r - H_w) \quad (3)$$

In this case, the quantities with subscript * are evaluated at a reference enthalpy given by

$$h^* = 0.5(h_e + h_w) + 0.22(h_r - h_e) \quad (4)$$

The local static pressure is the primary factor determining the predicted heat-transfer rates, because all of the relevant fluid properties are calculated by assuming isentropic expansion from the freestream conditions to the measured static pressure. By inspection of Eqs. (1) and (3), it is noted that pressure augments the heat transfer through its effect on the density and reduces it through the Reynolds number dependency.

When the coupled effects of the pressure and temperature (assuming an isentropic relationship) on the viscosity and density are considered, it can be shown that, for a specific heat ratio of 1.4, turbulent heating rates vary as the pressure to the power of 0.6 and laminar rates to the power of 0.43. Comparing the shape of the pressure and heat-transfer profiles can therefore, in principle, be used as a means of determining whether the boundary layer is laminar or turbulent. However, this technique was not found useful here, possibly because some of the pressure disturbances appeared to induce transition effects.

Results

Laminar

The experimental heat-transfer and pressure profiles are shown in Fig. 3 for condition A in the long combustion chamber known to have a laminar boundary layer. The data are plotted against $Re_{x\infty}$, which is calculated using the intake conditions. The heating rates are seen to be mainly of the same order as the laminar predictions, but with an apparently anomolous peak in the middle of the fuel on trace (Fig. 3b). Any disturbance causing a departure from laminar flow would be expected to increase significantly with the Reynolds number rather than to revert to the laminar values, as observed here. However, this effect is occurring in a region of falling pressure known to have a stabilizing influence on the boundary layers. The data have been plotted in Fig. 4 using a Reynolds number Re_{xL} based on local conditions outside the boundary layer. It is seen that in regions of falling pressure the Reynolds number may, in fact, fall with distance due to the lower density. The fuel on profile as displayed in Fig. 4b is typical of a boundary layer approaching transition with an increasing Reynolds number. If this is so, then disturbances from the combustion region, which are not present for the fuel-off cases of Figs. 3a and 4a, would appear to be sending the boundary layer into transition. However, because of the favorable pressure gradient, it subsequently relaminarizes when clear of the disturbances. This is a condition that has not, to our knowledge, been reported before. An alternative explanation is that the compressive effects of the pressure disturbances on the boundary layer are not correctly modeled by Eq. (3) in regions of unfavorable pressure gradient.

The experiments were repeated for condition B, but over a wider range of Reynolds numbers by use of both the long and short combustion chambers. The results are plotted in Figs. 5 and 6 against freestream and locally based Reynolds numbers, respectively. The results for the long combustion chamber are very similar to the same configuration using condition A, as can be seen by comparing Fig. 4b with the right-hand side of Fig. 6b. The results from the short combustion chamber show the same general trend, on a freestream Reynolds number basis, when compared to condition A with a long combustion chamber. These two conditions overlapped in Reynolds number and the similarity is seen by comparing Figs. 3a and

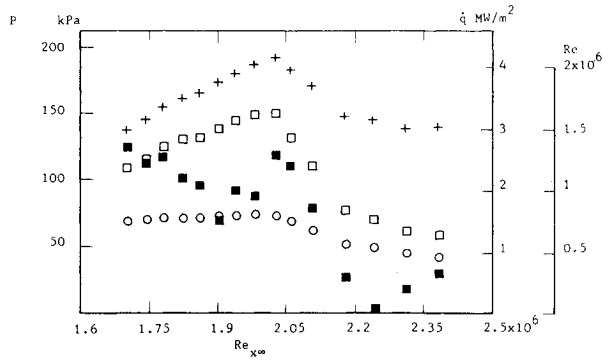

a) Fuel off.

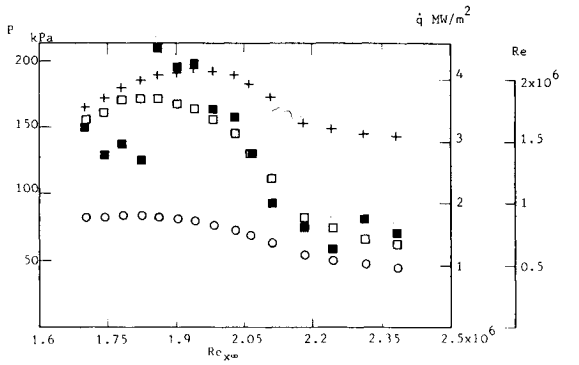

b) Fuel on.

Fig. 3 Long combustion chamber with diverging nozzle, condition A (□ P, ■ $\dot{q}$ experimental, ○ $\dot{q}$ laminar theory, ● $\dot{q}$ turbulent theory, + Re_{xL}).

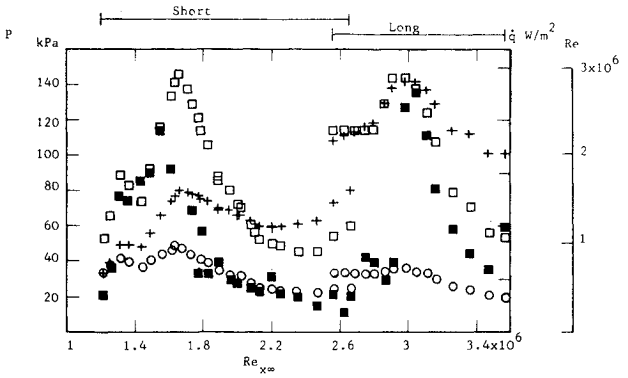

a) Fuel off.

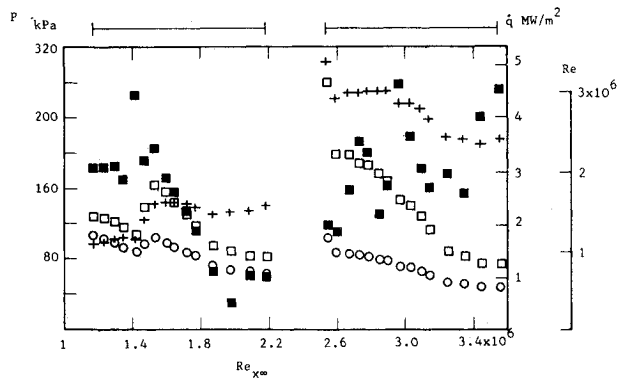

b) Fuel on.

Fig. 5 Long and short combustion chambers with diverging nozzle, condition B (see Fig. 3 for definitions of symbols).

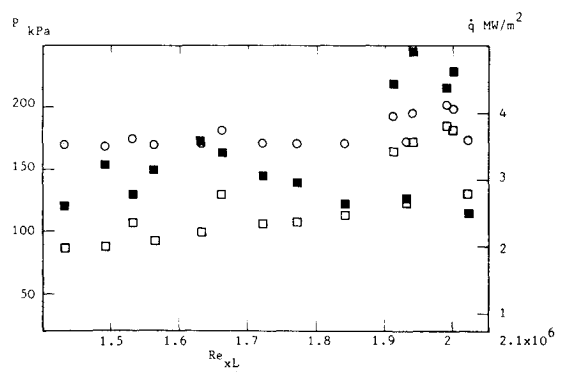

a) Fuel off.

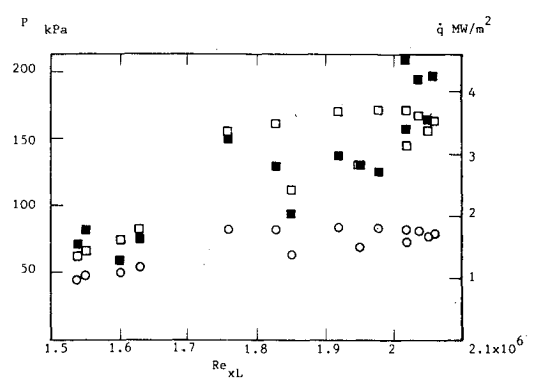

b) Fuel on.

Fig. 4 Long combustion chamber with diverging nozzle, condition A (see Fig. 3 for definitions of symbols).

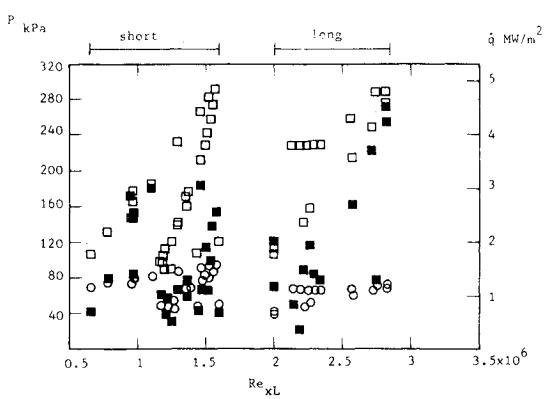

a) Fuel off.

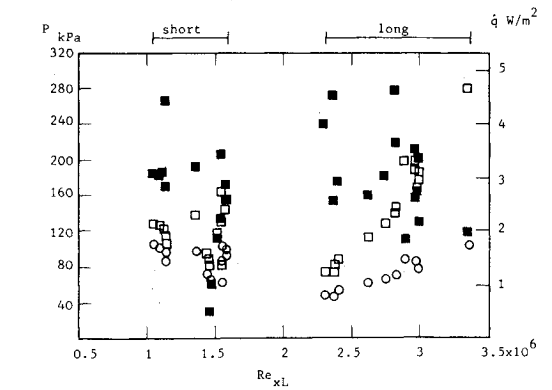

b) Fuel on.

Fig. 6 Long and short combustion chambers with diverging nozzle, condition B (see Fig. 3 for definitions of symbols).

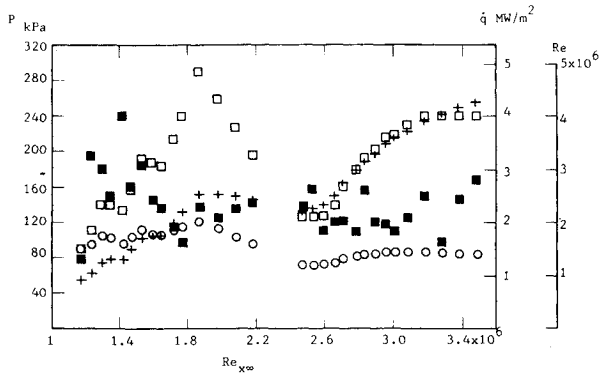

a) Fuel off.

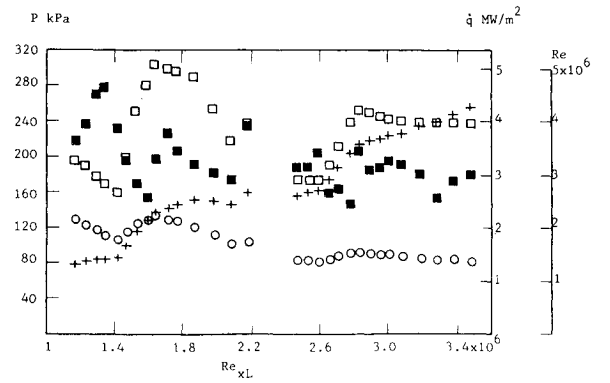

b) Fuel on.

Fig. 7 Constant-area duct, condition B (see Fig. 3 for definitions of symbols).

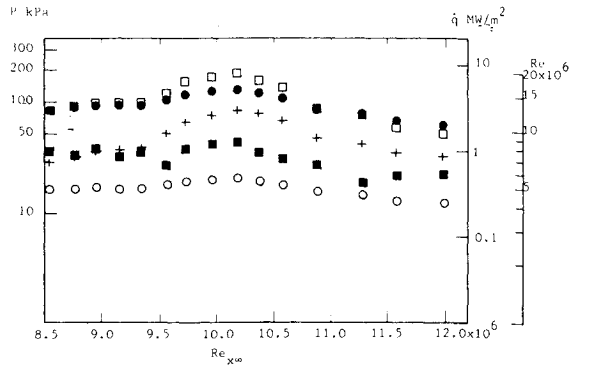

a) Fuel off.

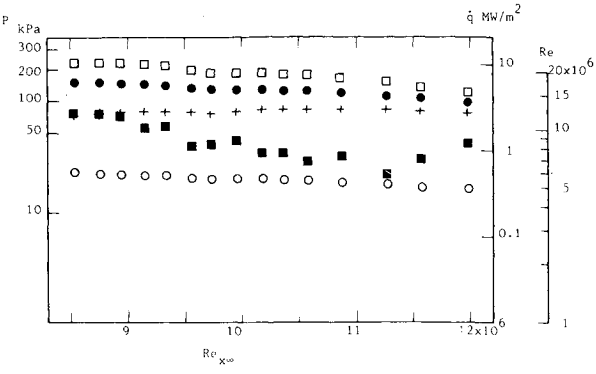

b) Fuel on.

Fig. 8 Long combustion chamber with divergence, condition C (see Fig. 3 for definitions of symbols).

3b with the left-hand sides of Figs. 5a and 5b. However, when mapped onto a local Reynolds number display, the short combustion chamber does not show the consistent increase of heat transfer with Reynolds number characteristic of such transition. This is illustrated in the left half of Fig. 6b. There is a general shift of the higher heating rates to the higher Reynolds numbers, but the effect is inconsistent. This appears to indicate that the effect is not one of transition with subsequent relaminarization, but, as suggested above, a local interaction effect between compression waves and the boundary layer. In the short combustion chamber, the expansion is started further upstream in the development of the fuel/air mixing region and a different system of pressure waves is transmitted to the thrust surface. This may explain the difference between the two cases at the same Reynolds number.

For both cases, Fig. 3 and the left half of Fig. 5, the experimental results agree well with the laminar predictions in the downstream region where the fuel-on and fuel-off pressure levels are similar. These are all regions of favorable pressure gradient. This suggests that the pressure-corrected empirical correlations can be applied in regions of expansion, free of strong pressure waves from the combustion region, if the boundary layer is laminar. For the long combustion chamber, with condition B, the heat-transfer rate is seen from Figs. 5b and 6b to increase in a region of falling pressure, but increasing Reynolds number. This suggests that the effect is one of genuine transition, which is consistent with the increased Reynolds number. As there was no flow visualization for condition B, this cannot yet be confirmed.

To summarize the data discussed so far, the empirical laminar formula underestimate the heat transfer in regions where there is evidence of transition, as expected, and also in regions showing strong adverse pressure gradients. Several causes should be investigated for the second phenomenon:

1) Instrument error. Use of thin-film gages is a well-established technique and the calibration error should not exceed 15%, which is not enough to explain the observed effects.

2) Transport of combustion products to the boundary layer. The mixing process has been studied with a two-dimensional computer program,[17] which shows that combustion products have not reached the wall in significant concentrations in the instrumented region of the model. There are also regions of adverse pressure gradient for fuel-off runs that show the same effect, as may be seen from Figs. 5a and 3a.

3) Use of an entirely empirical formula that relates only to flat plates. There is no theoretical basis for expecting it to apply to a different geometry and an untried set of freestream conditions, which may be the reason for the lack of agreement. However, the correlation is good for much of the flow and can be used for preliminary estimates if the limits of its suitability can be determined.

4) Flame radiation. As mentioned above, the platinum gages absorb infrared radiation. Radiation emitted from the flame may therefore contribute to the indicated heat transfer. A pure hydrogen flame does not emit much radiation; however, impurities in the gas do and it is not known what the effective emissivity of the test gas is. "Worst-case" estimates, assuming black-body emissions from the reacting region, have been made by using the temperature predictions from the two-dimensional computer code. These are not able to explain the difference between fuel-on and fuel-off heating rates seen, for example, in Fig. 3. This difference is significantly greater than the experimental error and also greater than the differences in the theoretical values given by the local static pressures.

Radiation from the freestream could be significant for both fuel-on and fuel-off cases. This would be most significant for the high-enthalpy condition A, but it is seen from Fig. 3 that there are regions in the low-pressure end where the results agree with the predictions within the experimental accuracy. The static temperature in this expanded region is still greater

than 2600 K and it would, therefore, be radiating strongly if there were a significant number of emitting particles in the flow. It is not thought that radiation effects contribute to any of the deviations from flat-plate predictions.

A further set of results is presented in Fig. 7 for a constant-area duct with condition B. This is an interesting case as it is nominally a flat plate and because multiple reflections of compression waves within the duct produce alternating regions of positive and negative pressure gradients. Mixing and combustion are more complete for the constant-area case, thus making it more susceptible to radiation effects and combustion product diffusion. The results are presented vs only intake-based Reynolds number to avoid overlapping data points.

The same general trends seen in Figs. 3 and 6 are reproduced here. The fuel-off results follow closely to the laminar predictions with perturbations generally associated with unfavorable pressure changes. At higher Reynolds numbers, greater than 3.1×10^6, the heating rates are consistently higher than laminar in a region of constant pressure. This could be incipient transition, as seen at the same Reynolds number in Fig. 5b, although the heating rate is no higher than some of the upstream values and is very much lower than the turbulent levels. The fuel-on rates are higher than laminar throughout, with the peaks corresponding roughly to positive pressure gradients. There is no systematic deviation away from laminar values for a Reynolds number range of $1\text{–}3.5\times10^6$, despite local errors in regions of unfavorable pressure gradient.

Also shown in Figs. 3, 5, and 7 are the locally calculated Reynolds numbers Re_{xL}. Any increase in the measured heating rate over the predictions is generally associated with a rapid rise in Re_{xL} in an axial direction; however, adverse pressure gradients are a more reliable indicator of this transition. The heating rate will regain the laminar values only if there is a subsequent drop in Re_{xL}. This seems to be a more reliable indicator of the reverse change than the pressure gradient, as may be seen from Fig.7b where the fuel-on measurements do not reattach to the laminar values, despite a favorable pressure gradient between Reynolds numbers 1.6×10^6 and 2.2×10^6 based on the intake conditions. Over the same range, Re_{xL} increases from 2×10^6 to 2.66×10^6. A tentative conclusion seems to be that the heating rates will definitely be above laminar for adverse pressure gradients and will require a fall in the local Reynolds number in order to revert to laminar values.

Turbulent

Condition C, which was known to have a turbulent boundary layer, was tested with the long combustion chamber. The results from this are presented in Fig. 8 vs the intake-based Reynolds number. The data are plotted on a log scale to show that the heating rates are proportionately half-way between the laminar and turbulent predictions. The reason for this is not known, but it is assumed that either the boundary layer is still transitional or that the turbulent approximations do not apply under these conditions. The negative pressure gradient is such that the locally based Reynolds number is approximately constant for the fuel-on case. If the boundary layer was not fully turbulent by the start of the diverging section, it is possible that this would prevent fully turbulent flow from developing.

Conclusions

Flat-plate empirical correlations for cooled laminar boundary layers can be used to give order-of-magnitude estimates of the heat transfer in scramjet combustion chambers. The role of the locally based Reynolds number is not properly understood or modeled; however, if the local pressures are known or calculated, the regions in which the heat-transfer predictions will be inaccurate can be identified. Radiation heat transfer does not appear to be significant in the geometry chosen. Transition regions are hard to identify and the results for turbulent flow are incomplete and inconclusive at present.

Acknowledgments

This work was supported by the Australian Research Grants Scheme and NASA Contract NAGW-499. The help of the staff at the Department of Physics and Theoretical Physics, Australian National University, in providing the experimental facility is greatly appreciated.

References

[1]Carlson, C.H., "Preliminary Scramjet Design for Hypersonic Air Breathing Missile Application," NASA CR 3742, 1983.

[2]Guy, R.A. and Mackley, E.A., "Initial Wind Tunnel Tests at Mach 4 and 7 of a Hydrogen Burning, Air Frame Integrated Scramjet," Paper presented at 4th International Symposium on Air Breathing Engines, Lake Buena Vista, FL, April 1979.

[3]Stalker, R.J., *Aeronautical Journal,* Vol. 76, 1972, pp. 374-384.

[4]Hornung, H.G. and Stalker, R.J., "Studies of Relaxation Gas Dynamics in the Free Piston Shock Tunnel," *Applied Fluid Mechanics,* edited by H. Oertel Jr., Karlsruhe, 1978, pp. 19-28.

[5]Crane, K.C.A. and Stalker, R.J., "Mass-Spectrometric Analysis of Hypersonic Flows," *Journal of Physics D: Applied Physics,* Vol. 10, 1977, pp. 679-695.

[6]Stalker, R.J. and Morgan, R.G., "Supersonic Hydrogen Combustion with a Short Thrust Nozzle," *Combustion and Flame,* Vol. 57, No. 1, July 1984, pp. 55-70.

[7]Morgan, R.G. and Stalker, R.J., "Fast Acting Hydrogen Valve," *Journal of Physics E: Scientific Instruments,* Vol. 16, 1983, pp. 205-207.

[8]Allen, J.L., Oxford University, Oxford, England, private communication, 1982.

[9]Ligrani, P.M., Camci, C., and Grady, M.S., "Thin Film Heat Transfer Gage Construction and Measurement Details," Von Kármán Institute for Fluid Dynamics, Brussels, Tech. Memo. 33, 1982.

[10]Schultz, D.L. and Jones, T.V., "Heat Transfer Measurements," AGARDograph 165, 1973.

[11]Lordi, J.A., Mates, R.E., and Moselle, J.R., "Computer Program for the Numerical Solution of Nonequilibrium Expansions of Reacting Gas Mixtures," NASA CR 472, 1966.

[12]Lin, C.C. (ed.), "Turbulent Flows and Heat Transfer," *High Speed Aerodynamics and Jet Propulsion,* Vol. 5, Oxford University Press, London, 1959, pp. 396-399.

[13]Henderson, A. Jr., "Hypersonic Viscous Flows," *Modern Development in Gasdynamics,* Plenum Press, New York, 1969.

[14]Stollery, J.L. and Coleman, G.T., "A Correlation between Pressure and Heat Transfer Distributions at Supersonic and Hypersonic Speeds," *Aeronautical Quarterly,* Vol. 26, 1975, p. 304-315.

[15]Eckert, E.R.G., "Engineering Relations for Skin Frictions and Heat Transfer to Surface in High Velocity Flow," *Journal of the Aeronautical Sciences,* Vol. 22, 1955, p. 585.

[16]Hayes, W.D. and Probstein, R.F., *Hypersonic Flow Theory,* Academic Press, New York and London, 1959.

[17]Evans, J.C., Schexnayder, C.J. Jr., and Beach, H.L. Jr., "Application of a Two-Dimensional Parabolic Computer Program to Prediction of Turbulent Reacting Flow," NASA TP 1169, March 1978.